Biophysical Journal Volume 75 December 1998 2647–2657

Differences in Saxitoxin and Tetrodotoxin Binding Revealed by Mutagenesis of the Na^+ Channel Outer Vestibule

Jennifer L. Penzotti, Harry A. Fozzard, Gregory M. Lipkind, and Samuel C. Dudley, Jr.

Cardiac Electrophysiology Labs and the Departments of Pharmacological and Physiological Sciences and Biochemistry and Molecular Biology, University of Chicago, Chicago, Illinois 60637 USA

ABSTRACT The marine guanidinium toxins, saxitoxin (STX) and tetrodotoxin (TTX), have played crucial roles in the study of voltage-gated Na^+ channels. Because they have similar actions, sizes, and functional groups, they have been thought to associate with the channel in the same manner, and early mutational studies supported this idea. Recent experiments by Kirsch et al. (1994. *Biophys. J.* 67:2305–2315) have suggested that the toxins bind differently to the isoform-specific domain I Phe/Tyr/Cys location. In the adult skeletal muscle Na^+ channel isoform (μI), we compared the effects on both TTX and STX affinities of mutations in eight positions known to influence toxin binding. The results permitted the assignment of energies contributed by each amino acid to the binding reaction. For neutralizing mutations of Asp^{400}, Glu^{755}, and Lys^{1237}, all thought to be part of the selectivity filter of the channel, the loss of binding energy was identical for the two toxins. However, the loss of binding energy was quite different for vestibule residues considered to be more superficial. Specifically, STX affinity was reduced much more by neutralizations of Glu^{758} and Asp^{1532}. On the other hand, mutation of Tyr^{401} to Cys reduced TTX binding energy twice as much as it reduced STX binding energy. Kinetic analysis suggested that all outer vestibule residues tested interacted with both toxins early in the binding reaction (consistent with larger changes in the binding than unbinding rates) before the transition state and formation of the final bound complex. We propose a revised model of TTX and STX binding in the Na^+ channel outer vestibule in which the toxins have similar interactions at the selectivity filter, TTX has a stronger interaction with Tyr^{401}, and STX interacts more strongly with the more extracellular residues.

INTRODUCTION

The marine guanidinium toxins tetrodotoxin (TTX) and saxitoxin (STX) are specific high-affinity blocking ligands of voltage-dependent Na^+ channels. They have been invaluable in biochemical purification of the channels (Catterall, 1995), in pharmacological characterization of the different channel isoforms (Moczydlowski et al., 1986a), and in determination of the channel density in cells (Ritchie and Rogart, 1977). These toxins bind competitively to a site on the external surface of the channel, named toxin site 1 (Catterall, 1980, 1986, 1988). Terlau et al. (1991) have located this site to the SS1-SS2 segments of all four domains of the channel protein by demonstrating that several mutations in this region of the rat brain II Na^+ channel isoform altered binding affinities of STX and TTX. Furthermore, some of their mutants changed permeation and/or selectivity of the channel, leading Terlau et al. (1991) to propose an alignment of portions of the four segments (pore-forming or P loops), one from each of the four domains, that form the channel outer vestibule and toxin site 1. According to their alignment of the four P loops, an inner set of the residues Asp, Glu, Lys, and Ala (DEKA) formed the narrowest part of the pore and functioned as the selectivity filter. A more superficial or extracellular set of aligned residues was composed of Glu, Glu, Met, and Asp from domains I–IV, respectively. Subsequently, residues of both sets have been implicated in channel conductance, selectivity, or toxin binding (Noda et al., 1989; Terlau et al., 1991; Backx et al., 1992; L.-Q. Chen et al., 1992; Heinemann et al., 1992b; Kontis and Goldin, 1993; Stephan et al., 1994; Chiamvimonvat et al., 1996a,b; Favre et al., 1996; Pérez-García et al., 1996, 1997; Schlief et al., 1996; S. F. Chen et al., 1997; Sun et al., 1997; Tsushima et al., 1997).

TTX and STX are thought to bind to the channel in the same manner (Hille, 1975; Kao and Walker, 1982; Strichartz, 1984; Kao, 1986; Yang et al., 1992). This idea is based upon the fact that the two toxins completely block current, competitively inhibit each other in binding assays, are of similar size, and possess similar functional groups, including one or two guanidinium groups and a diol that are thought to be critically important for binding of either toxin. Furthermore, both toxins appear to block at the same depth within the electric field when the greater charge of STX is taken into account (Satin et al., 1994b), and mutations in the outer vestibule seem to have qualitatively similar effects on the affinities of both toxins (Noda et al., 1989; Terlau et al., 1991; Kontis and Goldin, 1993; Stephan et al., 1994). These similarities led Lipkind and Fozzard (1994) to propose a specific molecular model of the TTX and STX binding site based upon one guanidinium group of each toxin binding to the selectivity region in an identical manner.

The idea that STX and TTX bind in the same manner is reinforced by experiments suggesting that a single site in the

Received for publication 30 September 1997 and in final form 16 July 1998.

Address reprint requests to Dr. Samuel C. Dudley, Jr., Division of Cardiology, Emory University/VAMC, 1670 Clairmont Rd. (111B), Decatur, GA 30033. Tel.: 404-327-4019; Fax: 404-329-2211; E-mail: sdudley@emory.edu.

Dr. Dudley's present address is Division of Cardiology, Emory University, Atlanta, GA 30322.

0006-3495/98/12/2647/11 $2.00

domain I pore-forming region is responsible for the known isoform differences in STX and TTX affinities (Backx et al., 1992; L.-Q. Chen et al., 1992; Heinemann et al., 1992a; Satin et al., 1992, 1994a; Kirsch et al., 1994; Favre et al., 1995; Pérez-García et al., 1996). STX and TTX bind to cardiac Na^+ channels with an ~25–100-fold lower affinity than to nerve or skeletal muscle channels. The lower affinity for both toxins in the cardiac isoform is thought to be the result of a Cys for Phe or Tyr substitution in domain I of the outer vestibule, which gives the cardiac Na^+ channel its distinctive phenotype of a reduced sensitivity to STX and TTX and an increased sensitivity to group IIb metals and Ca^{2+}. This difference in TTX affinity was reproduced in the Lipkind-Fozzard model (Lipkind and Fozzard, 1994) when an aromatic residue was substituted for Cys and TTX affinity increased by 4–5 kcal/mol.

Recently the hypothesis that STX and TTX bind in the same manner has been challenged by Kirsch et al. (1994), who demonstrated that the sulfhydryl reagent (2-aminoethyl)methanethiosulfonate (MTSEA) could decrease conduction of the human cardiac Na^+ channel (hH1a) by formation of a disulfide bond with the Cys in domain I of the pore. When bound to the channel, TTX protected Cys^{373} of hH1a from reaction with MTSEA, but STX did not, implying different binding arrangements for TTX and STX, at least for the region surrounding the Cys residue. In addition, Kontis and Goldin (1993) found that mutation of the outer ring glutamate of domain II in the rat brain IIA isoform had a larger effect on STX binding than on TTX binding. To determine differences in the specific interactions between the channel vestibule and the toxins, a quantitative comparison under identical conditions of the effects of mutations on both toxins is necessary. If they are bound in the same manner, then each mutation should produce an equivalent affinity change for both toxins. We studied the effects on TTX and STX affinities of mutations at eight important vestibule sites in the skeletal muscle Na^+ channel α-subunit (μI) expressed in *Xenopus* oocytes. To consider the mechanisms of differences in mutation effects and as a check on the IC_{50} measurements, we also measured the time courses of onset and offset of block.

A clear pattern emerged from these studies. First, the changes in binding energy (ΔG) for TTX and STX were almost identical for mutations of Asp^{400}, Glu^{755}, and Lys^{1237}, the tested residues from the selectivity region. The largest ΔG was for E755A of 5.4–5.7 kcal/mol. We concluded that the two toxins bind in a similar way to the selectivity region, and this was probably the mechanism of their block. Second, the effects of mutations of the more superficial set of charged residues were markedly different for TTX and STX. They showed the same change in energy when Glu^{403} was neutralized (ΔG = 5.2–6.2 kcal/mol), but the binding energy changes with mutations of Glu^{758} and Asp^{1532} were twice as large for STX (ΔG = 6.0–6.2 kcal/mol) as for TTX (ΔG = 2.4–3.3 kcal/mol). This suggested that a functional group not present in TTX, probably the second guanidinium of STX, interacted with the channel at this more extracellular location. Finally, mutation of Tyr^{401} to Cys caused twice the loss of binding energy for TTX than for STX (4.8 versus 2.7 kcal/mol). Based on these experimental data, adjustments in the positions of TTX and STX within the previously published outer vestibule model were able to explain many of these experimental findings, including access of MTSEA to Cys^{401} in the presence of STX.

MATERIALS AND METHODS

Oligonucleotide-directed point mutations were introduced by one of the following methods: mutations D400A, Y401D, Y401C, M1240K, and M1240E by the Unique Site Elimination Mutagenesis Kit (Pharmacia Biotech, Piscataway, NJ), following the manufacturer's instructions; mutation E403Q by the Altered Sites System (Promega, Madison, WI), following the manufacturer's instructions; mutation E755A by two primer PCR; mutations K1237R and K1237A by three primer PCR (Bowman et al., 1990); and mutations D1532N and E758Q by four primer PCR (Higuchi, 1990). Oligonucleotides were designed with silent restriction site changes for rapid identification of mutants. Vectors consisting of either the adult rat skeletal muscle Na^+ channel (μI) coding sequence flanked by *Xenopus* globin 5′ and 3′ untranslated regions in the pAlter phagemid (Promega, Madison, WI) or subcloned portions of this construct were used as templates for mutagenesis. PCR fragments were isolated and subcloned into μI by using directional ligations. The presence of the intended mutations and the absence of inadvertent mutations were verified by DNA sequencing of the entire polymerized regions. The vectors were linearized by SalI digestion and transcribed with SP6 DNA-dependent RNA polymerase, using reagents from the mCAP RNA Capping Kit (Stratagene, La Jolla, CA). The μI construct was a gift from Dr. Randall Moorman. The human heart Na^+ channel (hH1a) was obtained as a gift from Dr. Hali Hartmann, linearized with *Hin*dIII, and transcribed with T7 DNA-dependent RNA polymerase in the same manner as for μI. All PCR reagents were obtained from Perkin-Elmer (Norwalk, CT), and all restriction endonucleases were purchased from New England Biolabs (Beverly, MA).

Stage V and VI *Xenopus* oocytes from female frogs (NASCO, Ft. Atkinson, WI) were isolated and washed with a solution consisting of 90 mM NaCl, 2.5 mM KCl, 1 mM $MgCl_2$, 1 mM NaH_2PO_4, and 5 mM HEPES, titrated to pH 7.6 with 1 N NaOH, treated with 2 mg/ml collagenase (Sigma, St. Louis, MO) for 1.5 h, and had their follicular layers removed manually. Using a Drummond microinjector (Broomall, PA), ~50–100 ng of cRNA was injected into each oocyte. Oocytes were incubated at 16°C for 12–72 h before examination in a solution consisting of 90 mM NaCl, 2.5 mM KCl, 1 mM $CaCl_2$, 1 mM $MgCl_2$, 1 mM NaH_2PO_4, 2.5 mM Na pyruvate, 100 μg/ml gentamicin (Gibco-BRL, Grand Island, NY), 50 U/ml nystatin (Sigma), and 5 mM HEPES titrated to pH 7.6 with 1 N NaOH.

Recordings were made in the two-electrode voltage-clamp configuration, using a Dagan CA-1 voltage clamp (Minneapolis, MN). Data were collected using pClamp6.3 software (Axon Instruments, Foster City, CA) at 71.4 kHz after low-pass filtration at 2 kHz (8 pole Bessel, −3 dB), except for recordings of the more rapidly gating hH1a that were low-pass filtered at 10 kHz. All recordings were obtained at room temperature (20–22°C). Electrodes were filled with 3 M KCl and had resistances between 0.3 and 0.6 MΩ. The bath was constructed to favor laminar flow, and oocytes were placed in the middle of the bath flow to ensure rapid and uniform changes in the toxin concentration in the vicinity of the oocyte. Bath flow was typically 500 μl/min. The bath solution exchange rate was estimated by determining the time course of change in peak I_{Na} for oocytes expressing hH1a with voltage steps at 5-s intervals during a change from 90 mM NaCl to 45 mM NaCl and back. The time courses of I_{Na} changes were well fitted by single exponentials with time constants of 15–18 s. Examples of recordings of the peak Na^+ currents during wash in and wash out of toxin are shown in Fig. 1. For the different mutations, the time constants of the onset of and the recovery from toxin block ranged from 35 to 101 s and 47 to 177 s, respectively. In control experiments, the time

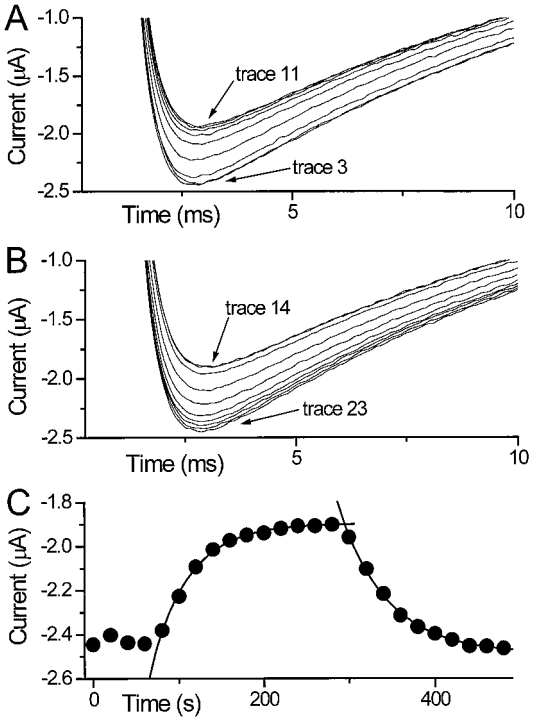

FIGURE 1 The method for determining the IC_{50} and kinetics of association and dissociation between toxins and the channel. In this example, *A* shows current traces recorded every 20 s at 0 mV from a holding potential of −100 mV before and during application of 1 nM STX to native μI Na^+ channels. The range on the ordinate has been adjusted to show that upon application of STX the peak currents decrease in an exponential manner. *B* shows the exponential recovery of the peak currents upon removal of STX. In *C*, the peak current amplitude is plotted as a function of time. Application of STX results in a time course of the decrease in the peak current that is well fitted by a single exponential. The recovery of peak current is also well fitted by a single exponential. The fitted exponential functions are shown as solid lines through the data. The time constants of these exponential functions can be used to calculate the toxin on and off rates as described in the text. In this case, the IC_{50}, K_d, k_{on}, and k_{off} are 3.6 nM, 7.3 nM, 2.48×10^6 M^{-1} s^{-1}, and 1.81×10^{-2} s^{-1}, respectively.

constants were not changed by doubling the solution flow rate. The effect of the bath exchange rate on the measured toxin blocking rate constants was calculated to result in a maximum error of less than twofold.

The standard bath solution consisted of 90 mM NaCl, 2.5 mM KCl, 1 mM $CaCl_2$, 1 mM $MgCl_2$, and 5 mM HEPES titrated to pH 7.2 with 1 N NaOH. Recordings made with K1237A used 1 mM $BaCl_2$ in place of $CaCl_2$, because mutation of this residue rendered the channel permeable to Ca^{2+} (Heinemann et al., 1992b; Favre et al., 1996; Schlief et al., 1996; S. F. Chen et al., 1997; Pérez-García et al., 1997; Sun et al., 1997; Tsushima et al., 1997), and upon channel activation in the presence of Ca^{2+}, a large outward current was induced. Control experiments in Ba^{2+}-containing solution with oocytes expressing wild-type μI showed no significant change in the equilibrium binding or kinetics measured under these conditions. STX and TTX were obtained from Calbiochem (La Jolla, CA). STX is shipped as a 1 mM stock solution in 100 mM acetic acid. Stock solutions of 3 mM TTX solution were made by diluting with distilled water. Stocks were stored at −20°C. Stored in this manner, toxin stock solutions showed no degradation over the course of these experiments. Toxin solutions of the desired concentrations were made by adding toxin stock solution to the standard bath solution and adjusting the pH to 7.2 with 1 N NaOH, as necessary.

The effect of toxin addition was monitored by recording the peak current elicited every 20 s upon step pulses to −20 mV, −10 mV, or 0 mV of 70 ms duration for hH1a, K1237A, and all other mutations, respectively. The holding potential was −100 mV, except in the case of hH1a, where the holding potential was adjusted to −120 mV to ensure full channel availability. With this protocol, the time course to complete equilibration with the toxin was observed, and the 20-s interpulse interval avoided the development of use-dependent toxin block. The change in peak current with time was well fitted by single-exponential functions for all combinations of toxins and channels. Fitting was performed using the simplex algorithm provided with the pClamp6.3 software. The IC_{50} for toxin binding was calculated from the ratio of peak currents in the absence and presence of toxin based on a single-site Langmuir absorption isotherm according to the formula $IC_{50} = [\text{toxin}](I_{toxin}/I_{max})/(1 - (I_{toxin}/I_{max}))$, where I_{toxin} is the equilibrium peak current in the presence of a given toxin concentration and I_{max} is the peak current under control conditions. The inverse of the time constant of toxin unbinding (τ_{off}) was taken as the rate constant, k_{off}. The pseudo-first-order rate constant, k_{on}, was calculated from the time constant of the decrease in peak current during association of the toxin (τ_{on}) by using the following formula: $k_{on} = 1/[\text{toxin}]*(1/\tau_{on} - 1/\tau_{off})$. A kinetically derived toxin dissociation constant was calculated ($K_d = k_{off}/k_{on}$) for comparison with the IC_{50}. Occasionally, the onset and relief of block did not follow an exponential time course, and those experiments were not included in further analysis. In those experiments where both the IC_{50}s and K_ds were calculated, they were found to be comparable. When practical, a ~50% inhibitory concentration of toxin was used to determine the IC_{50}. Only in cases in which the binding affinity was very low was it necessary to decrease the toxin concentration to clearly resolve the exponential time course for toxin binding.

Data are presented as means ± SEM. Statistical comparisons were performed using two-tailed Student's *t*-tests or one-way ANOVAs. ΔG was calculated as the difference in the average $RT\ln(IC_{50})$ for the wild-type and mutant channels ($\bar{x}-\bar{y}$), where *R* is the gas constant and *T* is temperature. The standard errors (SEs) for ΔG were estimated as the sum of the standard errors of the $RT\ln(IC_{50})$ averages. The standard error for the ratio of ΔGs was determined by the formula

$$SE = ((\bar{x}/\bar{y})^2[(SE\bar{x}/\bar{x})^2 + (SE\bar{y}/\bar{y})^2])^{1/2}.$$

Molecular modeling was performed with Biosym software (Biosym Technologies, San Diego, CA), operating on a Silicon Graphics Elan 4000 workstation (Mountain View, CA). All energy calculations were based on the Biosym consistent valence force field. Other details may be found in Lipkind and Fozzard (1994).

RESULTS

Choice of mutations and control measurements of Na^+ current characteristics

For descriptive convenience, we will refer to the mutated residues deep within the vestibule's electric field (Chiamvimonvat et al., 1996a) as the "inner ring" and those located more superficial as the "outer ring," acknowledging that residues in these "rings" originally proposed by Terlau et al. (1991) may not be at exactly the same depth. Mutations were carried out in these two rings and at position 401, the site that confers phenotypic differences in guanidinium toxin affinities. This residue is between these rings and will be discussed separately.

The outer ring charged residues Glu^{403}, Glu^{758}, and Asp^{1532} were neutralized by using the most conservative substitutions. Inconsistencies in previous reports concerning the importance of Met^{1240} in the outer ring of domain III to TTX binding prompted further investigation of this site. Previously in μI, mutation of the Met^{1240} to Cys caused a

small but statistically significant improvement in TTX binding (Pérez-García et al., 1996). However, Chen et al. (1997) reported that the Cys substitution at this site in hH1a produced a 10-fold reduction in affinity for TTX and had no effect on STX affinity, and the mutation of Met^{1240} to Gln in the brain II isoform resulted in an ~10-fold reduction in STX and TTX binding (Terlau et al., 1991). In the studies of Terlau et al. (1991), M1240K dramatically reduced affinity for both toxins. To seek further insight into the role of this residue in STX and TTX binding, Met^{1240} was mutated to the positively charged Lys, which should electrostatically reduce binding affinity for the positively charged toxin, and to the negatively charged Glu, which would increase affinity if the interactions were simply electrostatic in nature.

The charged residues located deeper in the vestibule that are known to affect TTX and STX affinity are Asp^{400}, Glu^{755}, and Lys^{1237}. Terlau et al. (1991) found that, for domains I and II, conservative substitutions led to drastic reduction in single-channel conductance. Consequently, we chose to replace them with Ala, which is known to result in expressed whole-cell currents large enough to measure the toxin effects accurately (Favre et al., 1996; Sun et al., 1997). Finally, mutations of Tyr^{401}, the position analogous to Cys^{373} in hH1a, were undertaken to determine the nature of the interactions between this site and the toxins. This interaction was probed with two mutations substituting Tyr^{401} with the neutral Cys or with the charged Asp. Both mutations of μI have been shown previously to affect binding of one of the toxins (Backx et al., 1992; Favre et al., 1995; Pérez-García et al., 1996).

All mutants constructed and expressed in *Xenopus* oocytes showed voltage-dependent inward currents typical for Na^+ channels. The reversal potentials for only K1237A (2.6 ± 5.9 mV) and E755A (33.6 ± 0.7 mV) were significantly different from that in wild-type channels (45.5 ± 2.8 mV). Specifically, the reversal potential for the mutant D1532N was not different from that of wild-type channels. For K1237A, channel activation in Ca^{2+}-containing solutions induced a large outward current that usually resulted in the loss of voltage control. Substitution of Ba^{2+} for Ca^{2+} eliminated this outward current, so this current was presumed to be a Ca^{2+}-dependent Cl^- current induced by Ca^{2+} influx through Na^+ channels rendered nonselective by the K1237A mutation, but this phenomenon was not studied further.

Inner and outer ring residues significantly alter TTX affinity

Table 1 compares the effects of inner and outer ring mutations on the IC_{50}, k_{on}, and k_{off} for TTX block. The ratios of the IC_{50}s for the mutant and native μI channels are also shown. The IC_{50} for TTX block of native μI Na^+ channels in these experiments was similar to those reported for native skeletal muscle preparations (Pappone, 1980; Moczydlowski et al., 1984b; Guo et al., 1987) or for μI expressed heterologously in *Xenopus* oocytes (Trimmer et al., 1989; Backx et al., 1992; L.-Q. Chen et al., 1992; Satin et al., 1992; Stephan et al., 1994; Pérez-García et al., 1996). The calculated k_{on} and k_{off} were slower than those from native Na^+ channels reconstituted with batrachotoxin in lipid bilayers (French et al., 1984; Moczydlowski et al., 1984a,b, 1986b; Green et al., 1987; Guo et al., 1987), but were similar to those from the frog node of Ranvier after accounting for a slight difference in the K_ds of the two preparations (Ulbricht et al., 1986). Possible reasons for this variation are discussed later. K_d values calculated from the rate constants agreed well with the IC_{50} measurements, however.

Glu^{755} of domain II was the most important of the inner ring residues in determining the blocking efficacy of TTX. The rank order of importance of the domains for the inner ring residues was II $\gg$ III $>$ I. Neutralizations D400A, E755A, and K1237A from domains I, II, and III resulted in ΔGs of 3.3, 5.4, and 4.1 kcal/mol, respectively (see Table 4). These changes were associated primarily by decreases in the toxin k_{on}s. Only in the case of E755A was there a statistically distinguishable but small increase in the TTX k_{off} ($p = 0.026$).

The relative importance of the domains was different for the outer ring. Neutralizations in the outer ring showed the rank order of the domains in blocking efficacy to be I $\gg$ II $>$ IV, suggesting that Glu^{403} of domain I was of overriding importance to TTX affinity. E403Q showed the largest ΔG of 5.2 kcal/mol, with ΔGs of E758Q and D1532N much smaller at 3.3 and 2.4 kcal/mol, respectively (see Table 4). The k_{off}s of all of the mutants were statistically indistinguishable from each other or from the wild-type k_{off} ($p = 0.49$, ANOVA). Therefore, changes in the IC_{50}s when these three residues were mutated were associated entirely with decreases in k_{on}.

TABLE 1 Changes in the IC_{50}, k_{on}, and k_{off} for TTX observed with mutations of the inner and outer rings

Mutation	Equilibrium IC_{50} (μM)	n	k_{on} (M^{-1} s^{-1})	n	k_{off} (s^{-1})	n	IC_{50} ratio
Native μI	0.036 ± 0.006	10	$3.53 \times 10^5 \pm 5.66 \times 10^4$	9	$1.02 \times 10^{-2} \pm 1.82 \times 10^{-3}$	9	1
D400A	6.0 ± 0.7	7	$2.93 \times 10^2 \pm 9.15 \times 10^1$	3	$1.26 \times 10^{-2} \pm 8.21 \times 10^{-4}$	3	168
E403Q	161 ± 14	8	$2.48 \times 10^2 \pm 1.17 \times 10^2$	5	$1.57 \times 10^{-2} \pm 4.09 \times 10^{-3}$	5	4521
E755A	229 ± 21	6	$2.90 \times 10^2 \pm 8.12 \times 10^1$	6	$2.69 \times 10^{-2} \pm 5.41 \times 10^{-3}$	6	6412
E758Q	6.2 ± 0.3	8	$4.86 \times 10^3 \pm 1.01 \times 10^3$	4	$1.47 \times 10^{-2} \pm 3.46 \times 10^{-3}$	4	174
K1237A	23 ± 2	4	$1.62 \times 10^2 \pm 4.41 \times 10^1$	3	$1.49 \times 10^{-2} \pm 1.45 \times 10^{-3}$	3	641
M1240E	87 ± 5	7	$4.15 \times 10^2 \pm 1.23 \times 10^2$	6	$1.98 \times 10^{-2} \pm 2.88 \times 10^{-3}$	6	2433
M1240K	238 ± 17	5	$1.02 \times 10^2 \pm 2.09 \times 10^1$	3	$1.58 \times 10^{-2} \pm 4.82 \times 10^{-3}$	3	6678
D1532N	1.5 ± 0.2	19	$6.14 \times 10^3 \pm 2.40 \times 10^3$	8	$1.45 \times 10^{-2} \pm 2.54 \times 10^{-3}$	10	43

Both positively and negatively charged mutations at the Met^{1240} significantly worsened TTX blocking efficacy. M1240K resulted in a 5.4 kcal/mol ΔG, whereas M1240E resulted in a 4.8 kcal/mol change. As with the other mutations, the main cause of the reduction in the IC_{50}s with either mutation was a decrease in k_{on}.

Inner and outer ring residues also affect STX affinity

The effects of inner and outer ring mutations on the IC_{50}, k_{on}, and k_{off} for STX are shown in Table 2. The IC_{50} for STX block of native and heterologously expressed recombinant μI Na^+ channels was similar to that in previous reports (Barchi and Weigele, 1979; Moczydlowski et al., 1984b, 1986b; Guo et al., 1987; Satin et al., 1992; Stephan et al., 1994; Favre et al., 1995). The blocking kinetics were slower by a factor of 5 than those calculated from single-channel recordings of STX block of skeletal muscle channels reconstituted in bilayers (Moczydlowski et al., 1984b; Guo et al., 1987) and those reported by Favre et al. (1995) for μI expressed in *Xenopus* oocytes. The rate constants differed by less than twofold from those reported for Na^+ channels of the node of Ranvier, however (Ulbricht et al., 1986).

As seen for TTX, the inner ring mutations caused large changes in affinity. E755A caused the largest change in the IC_{50}, implying that this residue was most important for STX block efficacy. The rank order of importance of the domains for STX block was II $\gg$ III $\geq$ I, and neutralizations with Ala resulted in 5.7, 3.9, and 3.8 kcal/mol ΔGs for E755A, K1237A and D400A, respectively (see Table 4). These values are almost identical to the ΔGs for TTX blocking caused by these three mutations. As in TTX, kinetic analysis of STX showed that changes in the IC_{50}s observed with Ala substitutions resulted entirely from changes in the STX k_{on}s, with no change in the toxin k_{off}s. No statistically significant changes in the k_{off}s were observed with any of the mutations in the inner or outer rings ($p = 0.10$, ANOVA). As was seen in TTX, the k_{on}s for STX were significantly reduced by neutralizing the carboxyl groups Asp^{400} and Glu^{755}, as might be expected if these groups participated in electrostatic attraction of the toxin. Again, K1237A had the unexpected effect of decreasing the toxin k_{on} implying that the role of Lys^{1237} in toxin/channel association is not a simple electrostatic attraction of the Lys for the divalent, cationic STX. Supporting this assertion, K1237R appears to reduce the IC_{50} by 144-fold, suggesting that Lys in this position is crucial for optimum STX affinity (data not shown).

The outer ring amino acids played a more crucial role in STX affinity than in TTX affinity. Domains I, II, and IV appeared to be equally important for STX binding. For the mutations E403Q, D1532N, and E758Q, ΔGs were 6.2, 6.2, and 6.0 kcal/mol, respectively. These values were significantly different from those seen with TTX. As was seen for the inner ring, the loss of STX affinity was the result of changes in the toxin k_{on}s without significant changes in the k_{off}s.

As in TTX, charged mutations at Met^{1240} caused large changes in the IC_{50}s for STX. With M1240K, the ΔG was 6.1 kcal/mol. This result was qualitatively similar to the effect of the analogous mutation in the rat brain II channel (Terlau et al., 1991). The M1240E mutation resulted in a loss of blocking efficacy ($\Delta G = 3.9$ kcal/mol), but it was considerably less than that seen with M1240K. Comparison of the results of M1240K and M1240E leaves open the possibility of an electrostatic component to the interaction between Met^{1240} mutations and STX, but electrostatic considerations were insufficient to explain the entire effect of mutations at this site.

STX and TTX showed differences in their response to mutations at Tyr^{401}

In domain I, an additional site between the inner and outer rings is important for STX and TTX binding (Backx et al., 1992; L.-Q. Chen et al., 1992; Heinemann et al., 1992a; Satin et al., 1992, 1994a; Kirsch et al., 1994; Favre et al., 1995; Pérez-García et al., 1996). We investigated whether mutations at the Tyr^{401} site in μI had similar effects on both STX and TTX blocking kinetics and equilibrium affinity. The results were compared with those obtained with the human heart Na^+ channel, hH1a, which normally contains a Cys at this site.

Table 3 compares the IC_{50}s and kinetic parameters of TTX and STX blocking of the wild-type μI, Y401D, Y401C

TABLE 2 Changes in the IC_{50}, k_{on}, and k_{off} for STX observed with mutations of the inner and outer rings

Mutation	Equilibrium IC_{50} (μM)	n	k_{on} (M^{-1} s^{-1})	n	k_{off} (s^{-1})	n	IC_{50} ratio
Native μI	0.003 ± 0.0004	10	$5.13 \times 10^6 \pm 3.06 \times 10^6$	4	$1.34 \times 10^{-2} \pm 1.74 \times 10^{-3}$	4	1
D400A	1.9 ± 0.2	10	$1.60 \times 10^3 \pm 3.65 \times 10^2$	7	$1.02 \times 10^{-2} \pm 1.46 \times 10^{-3}$	7	627
E403Q	121 ± 15	9	$1.76 \times 10^2 \pm 5.38 \times 10^1$	4	$8.50 \times 10^{-3} \pm 2.47 \times 10^{-3}$	4	39292
E755A	55 ± 5	8	$8.63 \times 10^2 \pm 3.21 \times 10^2$	4	$1.84 \times 10^{-2} \pm 3.34 \times 10^{-3}$	4	17927
E758Q	89 ± 10	5	$4.26 \times 10^2 \pm 8.51 \times 10^1$	3	$1.09 \times 10^{-2} \pm 4.94 \times 10^{-3}$	3	29093
K1237A	2.8 ± 0.7	6	$3.68 \times 10^3 \pm 1.81 \times 10^3$	4	$2.16 \times 10^{-2} \pm 5.50 \times 10^{-3}$	4	902
M1240E	2.2 ± 0.2	6	$1.33 \times 10^4 \pm 7.89 \times 10^3$	5	$9.71 \times 10^{-3} \pm 2.83 \times 10^{-3}$	5	704
M1240K	103 ± 15	10	$2.25 \times 10^2 \pm 4.12 \times 10^1$	4	$1.75 \times 10^{-2} \pm 5.20 \times 10^{-3}$	4	33564
D1532N	117 ± 15	9	$1.68 \times 10^2 \pm 8.24 \times 10^1$	4	$1.49 \times 10^{-2} \pm 2.60 \times 10^{-3}$	4	38248

TABLE 3 Comparison of IC_{50}s and kinetic parameters in μI, Tyr^{401} mutants, and hH1a channels

	Equilibrium IC_{50} (μM)	*n*	k_{on} (M^{-1} s^{-1})	*n*	k_{off} (s^{-1})	*n*	IC_{50} ratio
TTX							
Native μI	0.036 ± 0.006	10	$3.53 \times 10^5 \pm 5.66 \times 10^4$	9	$1.02 \times 10^{-2} \pm 1.82 \times 10^{-3}$	9	1
Y401D	171 ± 15	9	$3.03 \times 10^2 \pm 2.49 \times 10^2$	3	$1.42 \times 10^{-2} \pm 5.36 \times 10^{-3}$	3	4800
Y401C	80 ± 15	6	$8.77 \times 10^2 \pm 2.29 \times 10^2$	4	$2.60 \times 10^{-2} \pm 7.54 \times 10^{-4}$	4	2249
hH1a	1.5 ± 0.2	4	$4.41 \times 10^3 \pm 8.61 \times 10^2$	4	$2.11 \times 10^{-2} \pm 7.49 \times 10^{-4}$	4	41
STX							
Native μI	3.1 ± 0.4	10	$5.13 \times 10^6 \pm 3.06 \times 10^6$	4	$1.34 \times 10^{-2} \pm 1.74 \times 10^{-3}$	4	1
Y401D	169 ± 14	10	$2.41 \times 10^4 \pm 6.23 \times 10^3$	6	$7.10 \times 10^{-3} \pm 5.14 \times 10^{-4}$	6	55
Y401C	314 ± 12	5	$6.51 \times 10^4 \pm 1.43 \times 10^4$	4	$2.18 \times 10^{-2} \pm 3.44 \times 10^{-3}$	4	102
hH1a	149 ± 18	6	$9.50 \times 10^4 \pm 4.35 \times 10^4$	5	$9.09 \times 10^{-3} \pm 5.19 \times 10^{-4}$	5	48

and the human heart channels. As noted before, the blocking efficacy of TTX was lower in the hH1a channel as compared to μI, and this was mainfested by differences in both k_{on} and k_{off}. The IC_{50} for TTX block of hH1a was ~40-fold higher than that for μI and was on the order of previously reported values (Kirsch et al., 1994; Dumaine and Hartmann, 1996). Single-channel kinetics in batrachotoxin-modified channels showed qualitatively similar relationships of the TTX binding to skeletal and heart muscle channels, with a 30-fold difference in TTX blocking efficacy (Guo et al., 1987).

The Y401C mutation of μI did not reproduce the IC_{50} seen in hH1a, even though the mutation rendered all of the amino acids between and including the inner and outer rings the same as those in hH1a. Specifically, the IC_{50}s for TTX block of hH1a and μI-Y401C were, respectively, 40- and 2250-fold greater than μI. Backx et al. (1992) and Pérez-García et al. (1996) reported a similar difference in TTX affinity between μI-Y401C and the rat cardiac channel. Moreover, the mutation of Phe to Cys in the analogous position rendered the rat brain II Na^+ channel insensitive to 10 μM TTX (Heinemann et al., 1992a).

Favre et al. (1995) reported that Y401D bound STX more strongly than Y401C. Therefore, it was anticipated that the Y401D mutation might electrostatically attract TTX and improve its blocking efficacy. This was not the case, however. The Y401D mutation resulted in a 5.2 kcal/mol ΔG for TTX, as compared to a 4.8 kcal/mol ΔG with Y401C (see Table 4). This difference suggested that there was an even lower affinity for TTX when Asp was present in this position than with the Cys substitution.

TABLE 4 Changes in equilibrium binding free energy of STX and TTX for the outer vestibule mutants

Mutation	ΔG_{STX} ± SE	ΔG_{TTX} ± SE	$\Delta G_{STX}/\Delta G_{TTX}$ ± SE
D400A	3.8 ± 0.1	3.3 ± 0.3	1.2 ± 0.1
Y401D	2.4 ± 0.1	5.2 ± 0.3	0.5 ± 0.2
Y401C	2.7 ± 0.1	4.8 ± 0.3	0.6 ± 0.1
E403Q	6.2 ± 0.1	5.2 ± 0.3	1.2 ± 0.05
E755A	5.7 ± 0.1	5.4 ± 0.3	1.1 ± 0.1
E758Q	6.0 ± 0.1	3.3 ± 0.3	1.8 ± 0.05
K1237A	3.9 ± 0.2	4.1 ± 0.3	1.0 ± 0.1
M1240E	3.9 ± 0.1	4.8 ± 0.3	0.8 ± 0.1
M1240K	6.1 ± 0.2	5.4 ± 0.3	1.1 ± 0.1
D1532N	6.2 ± 0.2	2.4 ± 0.3	2.6 ± 0.1

In contrast, mutations in the 401 position affected STX blocking efficacy much less than that of TTX. As compared with μI, the IC_{50}s for Y401C, Y401D, and hH1a were reduced by 102-, 55-, and 48-fold, respectively. STX preferred the presence of a negatively charged residue to that of Cys, and the IC_{50}s for Y401C and hH1a were in much closer agreement than those seen with TTX. The values for IC_{50} were similar but slightly higher than those reported by Favre et al. (1995). Furthermore, the findings agreed with a Cys substitution in the rat brain II Na^+ channel, where the IC_{50} was 410 nM (Heinemann et al., 1992a). As is the case with all of the outer vestibule mutations, the k_{on}s varied considerably, but the k_{off}s showed relatively less change. Only the k_{off} in the presence of Y401D was statistically different from that of μI ($p = 0.03$).

DISCUSSION

We have compared the change in binding energy of TTX and STX resulting from mutations of eight different sites in the Na^+ channel vestibule. This mutational analysis permitted testing of a model we had previously proposed for guanidinium toxin binding to the outer vestibule (Lipkind and Fozzard, 1994), which had been challenged by mutational (Kontis and Goldin, 1993) and channel modification studies (Kirsch et al., 1994). We found that mutations of the three charged residues in the inner ring DEKA motif associated with the selectivity region of the pore led to identical changes in binding of both TTX and STX. In contrast, mutations of more superficial residues showed substantial differences in their effects on binding of the two toxins. The isoform-specific residue at position 401 (Phe/Tyr/Cys) also showed different roles in toxin binding. This new information supports our general scheme for the guanidinium toxin binding site but necessitates changes in several aspects our original model. Furthermore, it demonstrates that the isoform amino acid differences at positions analogous to 401 are not sufficient to explain fully the channel phenotypic differences in toxin affinities.

Comparison of STX and TTX affinity changes with mutation

The free energy changes for blocking efficacy (ΔGs) of STX and TTX upon mutations of outer vestibule residues are shown in Table 4. Calculation of the $\Delta G_{STX}/\Delta G_{TTX}$ ratios for the effects of a particular mutation showed that some mutations resulted in the identical losses in the energy of interaction (ratio close to 1.0) and that others showed greater affinity change for TTX (ratio $\leq$ 0.6) or greater affinity change for STX (ratio $\geq$ 1.8).

Mutations of the three charged residues in the DEKA selectivity region caused almost identical energy changes for the two toxins. Glu^{755} showed a ΔG of 5.4–5.7 kcal/mol and was the most important residue for binding of either toxin. Kontis and Goldin (1993) measured an identical ΔG of 4.3 kcal/mol for TTX and STX with E942Q in the brain IIA channel isoform (the position in that isoform equivalent to Glu^{755}). We found that Asp^{400} neutralization showed a significantly smaller ΔG for both toxins of 3.3–3.8 kcal/mol. The effect of substituting an Ala for Lys^{1237} was 3.9–4.1 kcal/mol for the toxins, although the interpretation of this effect is unclear (see later). Similarly, Chen et al. (1997) found that K1418C (the comparable residue in hH1a) produced a 3.1–3.7 kcal/mol change, nearly the same for the two toxins. The similar energies of interaction of these three sites for TTX and STX imply that the two toxins bind to the DEKA region of the vestibule in a nearly identical manner. Because of the similar actions of the two toxins and the similar interactions in this region, it seems reasonable to propose that this represents the site of block by both toxins.

Although STX and TTX bound in an energetically comparable manner to the selectivity filter region, there were significant differences in the interaction of the toxins with the outer ring residues. E403Q showed the same ΔGs for both toxins, but both E758Q and D1532N showed much larger ΔGs for the STX interactions than for those of TTX. The larger ΔG for E758Q agrees with the measurements of Kontis and Goldin (1993) for the analogous brain IIA mutation, E945Q. They found ΔGs of 3.3 kcal/mol for TTX and 5.7 kcal/mol for STX. In addition, Terlau et al. (1991) found double the effect of D1717N (the mutation in brain II comparable to our D1532N) on STX blocking efficacy compared to that of TTX (1.7 versus >3.9 kcal/mol). Furthermore, for D1713C in hH1a (the location comparable to D1532N), Chen et al. (1997) found about twice the energy change for STX as for that of TTX with the same mutation. One explanation might be that a functional group on STX not available on TTX interacts at this level.

Simple electrostatic considerations appear inadequate to explain our observations. In the most simple electrostatic model, because STX has about twice the positive charge that TTX does, charge-changing mutations should have had double the effect on STX. This was not the case, however, and elimination of charges at Asp^{400} and Glu^{755} resulted in similar ΔGs for the two toxins. In addition, neutralization of Lys^{1237} should have increased affinity, but on the contrary, K1237A reduced STX and TTX affinity substantially and nearly equally. Finally, replacement of Met^{1240} with either a positive or a negative charge-reduced affinity for both toxins. These results are most easily explained if the measured ΔGs result from local interactions rather than through-space electrostatic interactions with larger portions of the toxins. Alternatively, the discussed mutations could alter the structure of the toxin binding site or the orientation of the toxins with the site in similar ways. The fact that, of the mutations discussed, only those of Glu^{755} and Lys^{1237} changed the reversal potential argues against large changes in the channel conformation with the other mutations.

Rate constants offer some insight into the nature of the toxin interactions

The K_d derived from our rate constants correlated well with the observed equilibrium IC_{50} for each mutation. Our rate constants were most similar to those measured for the frog node of Ranvier (Ulbricht et al., 1986) but were slower than rate constants from reconstituted skeletal muscle or brain channels from either canines or rats (French et al., 1984; Moczydlowski et al., 1984a,b, 1986b; Green et al., 1987; Guo et al., 1987). These differences may be a function of the voltage at which toxin binding was measured, of ionic conditions, of pH, or of the presence of batrachotoxin with the reconstituted channels. The relatively slow rate of solution change in our experiments may have affected these rate constants, but estimates suggested that any error from this source is not sufficient to explain the measurements, except for the measurement of k_{on} for the mutant Y401C. Under these circumstances, the rate constant measurements should be interpreted qualitatively.

Because the association rates of many small ligands are less than expected by diffusion alone, a second rate-limiting relaxation step of the ligand-receptor initial encounter complex has been proposed (Guo et al., 1987, 1993; Escobar et al., 1993). In our case, mutations of the outer vestibule dramatically altered the IC_{50} for toxin binding but caused small changes to the k_{off}s. Further analysis of the changes in rate constants was attempted using rate theory. The change in the free energy of the transition state upon channel mutation is a logarithmic function of the ratio of the rate constants, assuming there are no binding intermediates with energies lower than STX or TTX in free solution. The ratio of the change in free energy of the transition state ($\Delta G^{\#} = RT \ln[k'/k]$) to the change in energy of the equilibrium bound state ($\Delta G = RT \ln[IC_{50}'/IC_{50}]$) has been called ϕ and gives a estimate of the extent of interaction formation between a channel residue and the toxin at the transition state (Matouschek et al., 1989; Fersht et al., 1992). This analysis may be applied to either k_{on} or k_{off}, giving ϕ_{on} or ϕ_{off}, respectively. If the association and dissociation pathways follow the same reaction coordinate and a new transition state is not created by the mutation, then $\phi_{on} = 1 - \phi_{off}$.

The basic premise is that if an association interaction occurs early in binding, then both the energies of the transition and the equilibrium bound states should be affected similarly by alterations of the interaction. A more complete discussion of this analysis may be found in Chang et al. (1998).

ϕ_{off} was close to 0 and ϕ_{on} was $\sim$1 for all channel mutation/toxin combinations, indicating that the transition state energy for the dissociation reaction was not affected greatly by the channel mutations. The kinetic analysis suggested that the channel residues interacted early in the binding reaction with both toxins and dissociated late in the unbinding phase. In other words, the channel-toxin associations tested appeared to form before the highest energy state during the binding reaction. Formation of the transition and final bound states must require conformational changes or further interactions in at least one more step, as proposed by Guo et al. (1987).

Tyr^{401} is more important for TTX binding

Differences in the responses of STX and TTX to mutations at the Tyr^{401} site were the most dramatic. Whereas both toxins bound better in the presence of Tyr, the mutations tested had a much larger impact on TTX block than on STX block, consistent with the $\Delta G_{STX}/\Delta G_{TTX}$ ratios < 1 for Y401D and Y401C. Furthermore, STX appeared to prefer a negative charge at this site, whereas TTX blocking efficacy was worsened in the presence of Y401D. A possible explanation for the differences in responses of STX and TTX is that the TTX-domain I interaction has a more hydrophobic character. Consistent with this idea, substitution of either Gly or Ala decreases STX block by >1000 fold (Favre et al., 1995). Alternatively, Y401D could affect binding indirectly by distorting the positions of more critical channel residues, such as Glu^{758} or Asp^{1532}.

The reason why Y401C does not recapitulate the toxin affinity seen in the heart channel is not clear. Previous observations have suggested similar findings, and attribution of this effect to an Arg present in the heart channel one amino acid carboxy to the domain I outer ring Glu seems to be not entirely satisfactory (Terlau et al., 1991; Heinemann et al., 1992a; Satin et al., 1992; Favre et al., 1995).

A new proposal for the TTX and STX binding orientation

We speculate on the implications of these experimental results for the toxin orientations with respect to our previously proposed model of their binding site (Lipkind and Fozzard, 1994). The toxins seemed to bind differently at three sites, Tyr^{401}, Glu^{758}, and Asp^{1532}. Comparing the groups most important for toxin binding (Yang and Kao, 1992), STX has two guanidinium groups (positions 1, 2, 3 and 7, 8, 9) and a C12 hydrated ketone, as compared to a single 1,2,3 guanidinium group and a vicinal diol at the C9 and C10 sites for TTX. We attempted to dock STX and TTX independently by assigning these different functional groups to the channel sites showing differences in binding.

Based on the arguments of Kao and his co-workers (Yang and Kao, 1992) about the critical nature of the STX 7,8,9 and the TTX 1,2,3 guanidinium groups for toxin activity, these groups were reserved for interaction with the DEKA ring. Two distinct polar interactions with Glu^{758} and Asp^{1532} distinguished STX interactions from those of TTX. Because D1532N had the larger effect, we located the charged STX 1,2,3 guanidinium group at an optimal hydrogen bond distance from the Asp^{1532} side chain. This left the C12 hydrated ketone adjacent to Glu^{758}. After energy minimization, STX spanned the outer vestibule model between domains II and IV (Fig. 2 *A*), and the 7,8,9 guanidinium group (located perpendicular to the 1,2,3 guanidinium) was in immediate contact with Glu^{755}. The shift of the 7,8,9 guanidinium group toward domain II left a large space between STX and Cys at position 401 (Fig. 2 *B*), consistent with the accessibility of that site to a sulfhydryl reagent (Kirsch et al., 1994) and with the minimal effect of the Y401W mutation on STX affinity (Favre et al., 1995). The STX carbamoyl, known to be important for binding (Strichartz et al., 1995), interacted with Glu^{403} of domain I, and the nonpolar C10, C11 side faced Met^{1240} on domain III. With STX in this orientation, the model was able to simulate the effects of several mutations. The calculated changes in the interaction energies for Asp^{400} and Glu^{755} in the DEKA ring were -4.6 and -5.6 kcal/mol, compared to measured ΔGs of 3.8 and 5.6 kcal/mol, respectively. For the more extracellular Asp^{1532} and Glu^{758}, the calculated energies were -7.4 and -6.6 kcal/mol, compared to measured ΔGs of 6.2 and 6.0 kcal/mol. The calculated ΔG for Y401C was 2.8 kcal/mol, quite similar to our experimentally observed value of 2.7 kcal/mol.

With the TTX 1,2,3 guanidinium group located analogously to the 7,8,9 guanidinium group of STX, the optimal Tyr^{401}/TTX interaction occurred with van der Waals contacts with the nonpolar C4-C5-C7-C8 side of the toxin (Fig. 2 *D*). The calculated nonbonded interaction energy change with the Y401C mutation in this location was 4.4 kcal/mol (-5.7 kcal/mol interaction with Tyr^{401} and -1.3 kcal/mol with Cys^{401}), similar to the 4.8 kcal/mol measured experimentally. Moreover, the dense packing of TTX with domain I would interfere with interaction of the sulfhydryl reagents with a Cys in this location. This orientation of TTX resulted in the C9 and C10 hydroxyl groups being near Glu^{758} and the C11 hydroxyl group near Glu^{403} (Fig. 2 *C*). The calculated interaction energies of Asp^{400}, Glu^{755}, Glu^{758}, and Asp^{1532} with TTX were -3.6, -5.0, -3.6, and -2.2 kcal/mol, consistent with the experimental findings.

The model did not reproduce all experimental findings, however. Based on electrostatic considerations, the model predicted that the mutation K1237A should have bound the toxins with higher affinity because of the loss of a repulsive force. Similarly, the model failed to predict the effect of the M1240E mutation. Perhaps the mutations contribute in some way to the structural integrity of the binding site, or

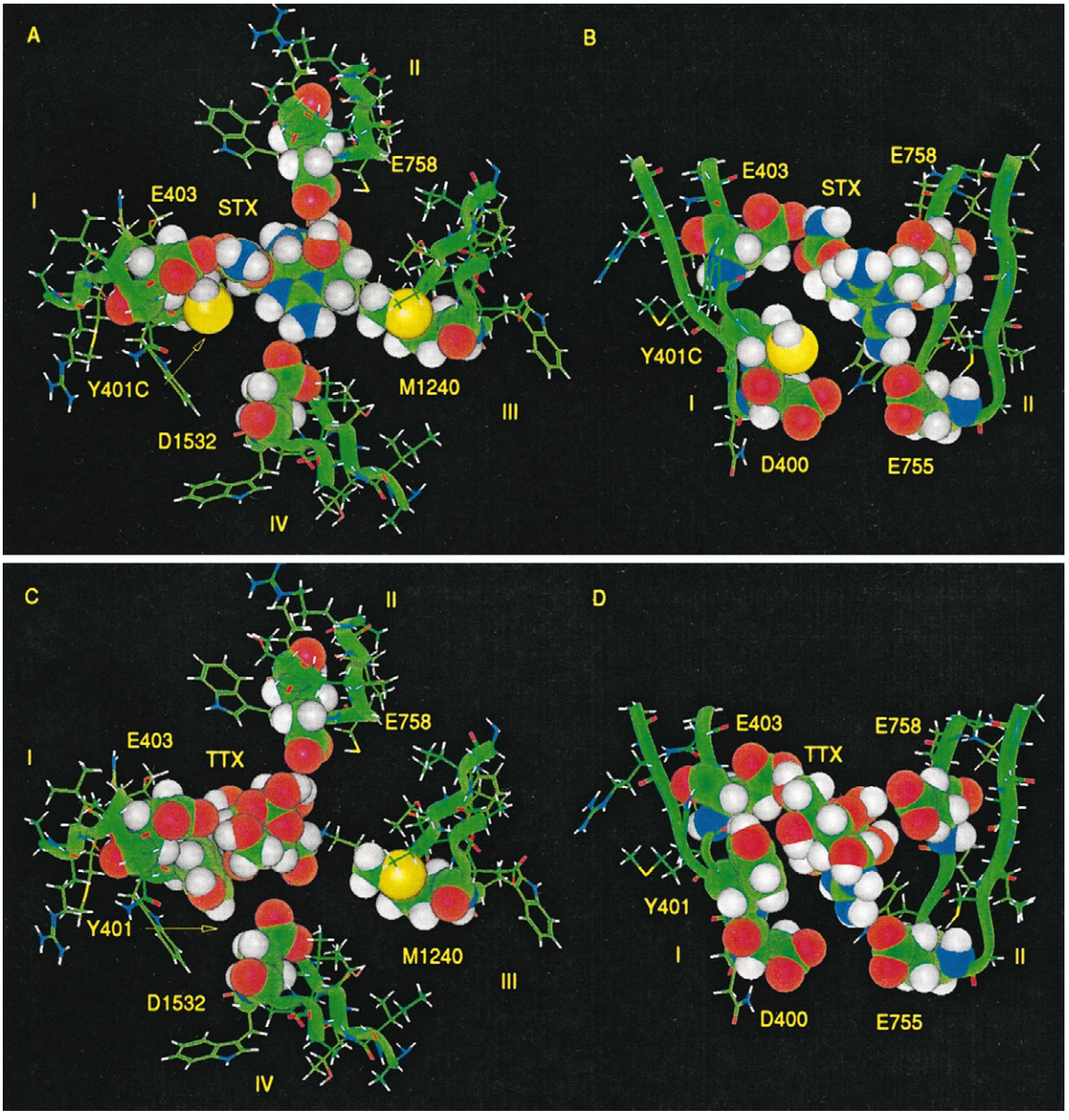

FIGURE 2 Proposed orientations of STX and TTX in a model of the μI Na^+ channel outer vestibule (Lipkind and Fozzard, 1994). The P loops are formed by β-hairpins, and their backbones are indicated by green ribbons. (*A*) Orientation of STX relative to domains I–IV, as viewed from the extracellular side down the axis of ion permeation, with the mutation Y401C present in domain I. The 1,2,3 guanidinium group is close to Asp^{1532} of domain IV, and the C12 diol interacts with Glu^{758} of domain II. In this orientation, the carbamoyl group of STX is near Glu^{403}. (*B*) Orientation of STX relative to domains I and II, viewed in a plane parallel to the membrane, showing the interaction of the 7,8,9 guanidinium with Glu^{755} and Asp^{400}. Because of its interaction with the outer ring, STX is held away from the 401 site, leaving room for sulfhydryl reagents to react with Cys in this position in the heart isoform. (*C*) Top view of the orientation of TTX with domains I–IV, showing the close packing of TTX with the domain I P loop. This packing would tend to prevent access of sulfhydryl reagents to the 401 site. (*D*) Side view of the orientation of TTX relative to domains I and II. The C4-C5-C7-C8 surface of TTX is closely packed with Tyr^{401}. Carbon, nitrogen, oxygen, and hydrogen are green, blue, red, and white, respectively.

the mutations create new, less favorable orientations of the toxins.

In summary, we performed a systematic assessment of the effects of mutations of the outer vestibule residues forming part of the guanidinium toxin binding site. The charged residues in the inner selectivity region interact similarly with STX and TTX, as demonstrated by the equivalent increases in the free energies of interaction of both toxins upon residue neutralization, supporting the conclusion that the two toxins block the pore by the same mechanism. Two outer ring residues, Glu^{758} and Asp^{1532}, were energetically more important for STX, however, because of the presence of the second guanidinium group. The residue at the 401 position was confirmed as an important, but not exclusive, contributor to the difference in guanidinium toxin affinity between the skeletal muscle and cardiac isoforms.

Distinctions in the response of toxins to mutations at the 401 site were noted, and modeling suggested that TTX might have a more intimate nonbonded interaction with domain I than STX, protecting this site from modification by sulfhydryl reagents. Our revised model was able to simulate the energies of interaction with six of the eight residues studied.

This research was supported by a Program Project Award from the National Institutes of Health (P01-HL20592-21), for which HAF is the principal investigator. JLP is a Howard Hughes Medical Institute Medical Student Research Training Fellow. The authors are indebted for the technical assistance provided by Ian Glaaser, Colleen Parrett, Yu Huang, and Bin Xu, and for the advice of Dr. Jack Kyle.

REFERENCES

Backx, P., D. Yue, J. Lawrence, E. Marban, and G. Tomaselli. 1992. Molecular localization of an ion-binding site within the pore of mammalian sodium channels. *Science.* 257:248–251.

Barchi, R. L., and J. B. Weigele. 1979. Characteristics of saxitoxin binding to the sodium channel of sarcolemma isolated from rat skeletal muscle. *J. Physiol. (Lond.).* 295:383–396.

Bowman, S., J. A. Tischfield, and P. J. Stambrook. 1990. An efficient and simplified method for producing site-directed mutations by PCR. *Technique.* 2:254–260.

Catterall, W. 1980. Neurotoxins that act on voltage-sensitive sodium channels in excitable membranes. *Annu. Rev. Pharmacol. Toxicol.* 20:15–43.

Catterall, W. A. 1986. Molecular properties of voltage-sensitive sodium channels. *Annu. Rev. Biochem.* 55:953–985.

Catterall, W. A. 1988. Structure and function of voltage-sensitive ion channels. *Science.* 242:50–61.

Catterall, W. A. 1995. Structure and function of voltage-gated ion channels. *Annu. Rev. Biochem.* 64:493–531.

Chang, N. S., R. J. French, G. M. Lipkind, H. A. Fozzard, and S. C. Dudley, Jr. 1998. Predominant interactions between μ-conotoxin Arg-13 and the skeletal muscle Na^+ channel localized by mutant cycle analysis. *Biochemistry.* 37:4407–4419.

Chen, L.-Q., M. Chahine, R. G. Kallen, R. L. Barchi, and R. Horn. 1992. Chimeric study of sodium channels from rat skeletal and cardiac muscle. *FEBS Lett.* 309:253–257.

Chen, S. F., H. A. Hartmann, and G. E. Kirsch. 1997. Cysteine mapping in the ion selectivity and toxin binding region of the cardiac Na^+ channel pore. *J. Membr. Biol.* 155:11–25.

Chiamvimonvat, N., M. T. Pérez-García, R. Ranjan, E. Marban, and G. F. Tomaselli. 1996a. Depth asymmetries of the pore-lining segments of the Na^+ channel revealed by cysteine mutagenesis. *Neuron.* 16:1037–1047.

Chiamvimonvat, N., M. T. Pérez-García, G. F. Tomaselli, and E. Marban. 1996b. Control of ion flux and selectivity by negatively charged residues in the outer mouth of rat sodium channels. *J. Physiol. (Lond.).* 491: 51–59.

Creighton, T. E. 1993. Proteins: Structures and Molecular Properties, 2nd Ed. W. H. Freeman and Co., New York. 344–346.

Dumaine, R., and H. Hartmann. 1996. Two conformational states involved in the use-dependent TTX blockade of human cardiac Na^+ channel. *Am. J. Physiol.* 270:H2029–H2037.

Escobar, L., M. J. Root, and R. MacKinnon. 1993. Influence of protein surface charge on the bimolecular kinetics of a potassium channel peptide inhibitor. *Biochemistry.* 32:6982–6987.

Favre, I., E. Moczydlowski, and L. Schild. 1995. Specificity for block by saxitoxin and divalent cations at a residue which determines sensitivity of sodium channel subtypes to guanidinium toxins. *J. Gen. Physiol.* 106:203–229.

Favre, I., E. Moczydlowski, and L. Schild. 1996. On the structural basis for ionic selectivity among Na^+, K^+, and Ca^{2+} in the voltage-gated sodium channel. *Biophys. J.* 71:3110–3125.

Fersht, A. R., A. Matouschek, and L. Serrano. 1992. I. Theory of protein engineering analysis of stability and pathway of protein folding. *J. Mol. Biol.* 224:771–782.

French, R. J., J. F. Worley, III, and B. K. Krueger. 1984. Voltage-dependent block by saxitoxin of sodium channels incorporated into planar lipid bilayers. *Biophys. J.* 45:301–310.

Green, W. N., L. B. Weiss, and O. S. Andersen. 1987. Batrachotoxin-modified sodium channels in planar lipid bilayers: characterization of saxitoxin- and tetrodotoxin-induced channel closures. *J. Gen. Physiol.* 89:873–903.

Guo, Z., A. Uehara, A. Ravindran, S. H. Bryant, S. Hall, and E. Moczydlowski. 1987. Kinetic basis for insensitivity to tetrodotoxin and saxitoxin in sodium channels of canine heart and denervated rat skeletal muscle. *Biochemistry.* 26:7346–7556.

Heinemann, S. H., H. Terlau, and K. Imoto. 1992a. Molecular basis for pharmacological differences between brain and cardiac sodium channels. *Pflügers Arch.* 422:90–92.

Heinemann, S. H., H. Terlau, W. Stühmer, K. Imoto, and S. Numa. 1992b. Calcium channel characteristics conferred on the sodium channel by single mutations. *Nature.* 356:441–443.

Higuchi, R. 1990. Recombinant PCR. *In* PCR Protocols: A Guide to Methods and Applications. M. A. Innis, editor. Academic Press, New York. 177–183.

Hille, B. 1975. The receptor for tetrodotoxin and saxitoxin. A structural hypothesis. *Biophys. J.* 15:615–619.

Kao, C. Y. 1986. Structure-activity relations of tetrodotoxin, saxitoxin and analogues. *Ann. N.Y. Acad. Sci.* 479:52–67.

Kao, C. Y., and S. E. Walker. 1982. Active groups of saxitoxin and tetrodotoxin as deduced from action of saxitoxin analogs on frog muscle and squid axon. *J. Physiol. (Lond.).* 323:619–637.

Kirsch, G. E., M. Alam, and H. A. Hartmann. 1994. Differential effects of sulfhydryl reagents on saxitoxin and tetrodotoxin block of voltage-dependent Na channels. *Biophys. J.* 67:2305–2315.

Kontis, K. J., and A. L. Goldin. 1993. Site-directed mutagenesis of the putative pore region of the rat IIA sodium channel. *Mol. Pharmacol.* 43:635–644.

Lipkind, G. M., and H. A. Fozzard. 1994. A structural model of the tetrodotoxin and saxitoxin binding site of the Na^+ channel. *Biophys. J.* 66:1–13.

Matouschek, A., J. T. Kellis, Jr., L. Serrano, and A. R. Fersht. 1989. Mapping the transition state and pathway of protein folding by protein engineering. *Nature.* 340:122–126.

Moczydlowski, E., S. S. Garber, and C. Miller. 1984a. Batrachotoxin-activated Na^+ channels in planar lipid bilayers: competition of tetrodotoxin block by Na^+. *J. Gen. Physiol.* 84:665–686.

Moczydlowski, E., S. Hall, S. S. Garber, G. S. Strichartz, and C. Miller. 1984b. Voltage-dependent blockade of muscle Na^+ channels by guanidinium toxins. Effects of toxin charge. *J. Gen. Physiol.* 84:687–704.

Moczydlowski, E., B. M. Olivera, W. R. Gray, and G. R. Strichartz. 1986a. Discrimination of muscle and neuronal Na-channel subtypes by binding competition between [^{3}H]saxitoxin and μ-conotoxins. *Proc. Natl. Acad. Sci. USA.* 83:5321–5325.

Moczydlowski, E., A. Uehara, X. Guo, and J. Heiny. 1986b. Isochannels and blocking modes of voltage-dependent sodium channels. *Ann. N.Y. Acad. Sci.* 479:269–292.

Noda, M., H. Suzuki, S. Numa, and W. Stühmer. 1989. A single point mutation confers tetrodotoxin and saxitoxin insensitivity on the sodium channel-II. *FEBS Lett.* 259:213–216.

Pappone, P. A. 1980. Voltage-clamp experiments in normal and denervated mammalian skeletal muscle fibres. *J. Physiol. (Lond.).* 306:377–410.

Pérez-García, M. T., N. Chiamvimonvat, E. Marban, and G. F. Tomaselli. 1996. Structure of the sodium channel pore revealed by serial cysteine mutagenesis. *Proc. Natl. Acad. Sci. USA.* 93:300–304.

Pérez-García, M. T., N. Chiamvimonvat, R. Ranjan, J. R. Balser, G. F. Tomaselli, and E. Marban. 1997. Mechanisms of sodium/calcium selectivity in sodium channels probed by cysteine mutagenesis and sulfhydryl modification. *Biophys. J.* 72:989–996.

Ritchie, J. M., and R. B. Rogart. 1977. The binding of saxitoxin and tetrodotoxin to excitable tissue. *Rev. Physiol. Biochem. Pharmacol.* 79:1–50.

Satin, J., J. W. Kyle, M. Chen, P. Bell, L. L. Cribbs, H. A. Fozzard, and R. B. Rogart. 1992. A mutant of TTX-resistant cardiac sodium channels with TTX-sensitive properties. *Science.* 256:1202–1205.

Satin, J., J. W. Kyle, Z. Fan, R. Rogart, H. A. Fozzard, and J. C. Makielski. 1994a. Post-repolarization block of cloned sodium channels by saxitoxin: the contribution of pore-region amino acids. *Biophys. J.* 66:1353–1363.

Satin, J., J. T. Limberis, J. W. Kyle, R. B. Rogart, and H. A. Fozzard. 1994b. The saxitoxin/tetrodotoxin binding site on the cloned rat brain IIa Na channel is in the transmembrane electric field. *Biophys. J.* 67: 1007–1014.

Schlief, T., R. Schonherr, K. Imoto, and S. H. Heinemann. 1996. Pore properties of rat brain II sodium channels mutated in the selectivity filter domain. *Eur. Biophys. J.* 25:75–91.

Stephan, M. M., J. F. Potts, and W. S. Agnew. 1994. The μI skeletal muscle sodium channel: mutation E403Q eliminates sensitivity to tetrodotoxin but not to μ-conotoxins GIIIA and GIIIB. *J. Membr. Biol.* 137:1–8.

Strichartz, G. 1984. Structural determinants of the affinity of saxitoxin for neuronal sodium channels. *J. Gen. Physiol.* 84:281–305.

Strichartz, G., S. Hall, B. Magnani, C. Hong, Y. Kishi, and J. Debin. 1995. The potencies of synthetic analogues of saxitoxin and the absolute stereoselectivity of decarbamoyl saxitoxin. *Toxicon.* 33:723–737.

Sun, Y. M., I. Favre, L. Schild, and E. Moczydlowski. 1997. On the structural basis for size-selective permeation of organic cations through the voltage-gated sodium channel. Effect of alanine mutations at the DEKA locus on selectivity, inhibition by Ca^{2+} and H^{+}, and molecular sieving. *J. Gen. Physiol.* 110:693–715.

Terlau, H., S. H. Heinemann, W. Stühmer, M. Pusch, F. Conti, K. Imoto, and S. Numa. 1991. Mapping the site of block by tetrodotoxin and saxitoxin of sodium channel-II. *FEBS Lett.* 293:93–96.

Trimmer, J. S., S. S. Cooperman, S. A. Tomiko, J. Zhou, S. M. Crean, R. L. Barchi, F. J. Sigworth, R. H. Goodman, W. S. Agnew, and G. Mandel. 1989. Primary structure and functional expression of a mammalian skeletal muscle sodium channel. *Neuron.* 3:33–49.

Tsushima, R. G., R. A. Li, and P. H. Backx. 1997. Altered ionic selectivity of the sodium channel revealed by cysteine mutations within the pore. *J. Gen. Physiol.* 109:463–475.

Ulbricht, W., H. H. Wagner, and J. Schmidtmayer. 1986. Kinetics of TTX-STX block of sodium channels. *Ann. N.Y. Acad. Sci.* 479:68–83.

Yang, L., and C. Y. Kao. 1992. Actions of chiriquitoxin on frog skeletal muscle fibers and implications for the tetrodotoxin/saxitoxin receptor. *J. Gen. Physiol.* 100:609–622.

Yang, L., C. Kao, and Y. Oshima. 1992. Actions of decarbamoyloxsaxitoxin and decarbamoylneosaxitoxin on the frog skeletal muscle fiber. *Toxicon.* 30:645–652.